

Crystal structures of Ti, Zr, and Hf under compression: Theory

Rajeev Ahuja

Department of Physics, Uppsala University, Box 530, Uppsala, Sweden

John M. Wills

Theoretical Division, Los Alamos National Laboratory, Los Alamos, New Mexico 87545

Börje Johansson and Olle Eriksson

Department of Physics, Uppsala University, Box 530, Uppsala, Sweden

(Received 6 July 1993)

We have studied the crystal structures of Ti, Zr, and Hf under pressure by means of first-principles, total-energy calculations. The three metals are shown to exhibit a crystal structure sequence $hcp \rightarrow \omega \rightarrow bcc$, with increasing pressure. This is in good agreement with experiment for Zr and Hf, whereas the bcc structure for Ti is a prediction. The calculated transition volumes as well as transition pressures compare fairly well with experiment. Also, the computed c/a ratio for hcp Ti, Zr, and Hf is found to be in good agreement with experiment. Similarly the calculated c/a ratio for Zr in the ω structure agrees well with measurement. The chemical bonding of the ω structure is shown to be quite different from what is normally the case in the transition metals, with a large degree of covalency. A search for the ω structure in Tc and Ru was fruitless yielding a stable hcp structure. At zero temperature and zero pressure the bcc crystal structure is found to be mechanically unstable for Ti, Zr, and Hf.

I. INTRODUCTION

It is well known that the titanium group of elements (Ti, Zr, and Hf) all have the hcp crystal structure at room temperature and zero pressure.¹ At high temperature and zero pressure they transform to the bcc structure before reaching the melting temperature. At room temperature and under pressure they undergo a crystallographic phase change into the so-called ω structure. At even higher pressures both Zr and Hf have been observed to transform to the bcc structure. Apparently there is a close correspondence between these three metals and in the present paper this will be investigated theoretically.

Various room-temperature experiments for Ti have shown a transition from hcp to the ω phase at a pressure of 119 kbar,² 20–70 kbar,³ 29–75 kbar,⁴ or 80 kbar.⁵ The ω phase remains stable in Ti up to the highest studied pressure, 870 kbar.⁵ In Zr the ω phase is stabilized by a pressure of 21–60 kbar (Ref. 3) or at 22 kbar.⁵ The c/a ratio of the ω phase in Zr was also investigated as a function of volume and was found to be almost constant, 0.625.⁵ The bcc structure was reported for Zr at a pressure of 300 kbar.⁵ Furthermore, Hf has also been investigated at room temperature as a function of pressure. Similar to the other elements in the Ti group the hcp structure is stable in Hf at low pressures but at a pressure of 380 kbar the ω phase is obtained, and finally the bcc structure is found to appear at 710 kbar.⁵ Thus, experimental data at room temperature show an interesting crystal structure sequence $hcp \rightarrow \omega \rightarrow bcc$, with increasing pressure, for Zr and Hf. For Ti the corresponding high-pressure bcc phase has not yet been observed, but it seems reasonable to expect that also for Ti the bcc structure will be stabilized at sufficiently large pressures. One

purpose of the present paper is to use theory to predict that Ti will crystallize in the bcc structure at high compressions.

The ω phase has an interesting crystal structure, a hexagonal lattice with three atoms per unit cell. The atomic positions are at $(0,0,0)$, $(\frac{1}{3}, \frac{2}{3}, c/2a)$, and $(\frac{2}{3}, \frac{1}{3}, c/2a)$, where the c/a ratio is ~ 0.62 . Thus, the symmetry of the crystal is high, there are 24 point-group operations, the same as for a simple hexagonal lattice.⁶ The ω phase has a quite open structure and the packing ratio (~ 0.57) is slightly larger than that of the simple cubic lattice (~ 0.52), but substantially lower than for the bcc (~ 0.68), fcc, or hcp structures (~ 0.74).

The occurrence of such an open structure in metals with metallic d bonding is quite unusual. Normally, the transition metals have fcc, hcp, or bcc structures and these close-packed (fcc and hcp) or fairly close-packed (bcc) structures are thought to be favored over more open, low-symmetry structures due to the Madelung contribution to the total energy. Among the close-packed structures the stability of a specific atomic geometry (fcc, hcp, or bcc) is known to be correlated with the number of d electrons.^{7–9} Namely, the crystal structure sequence, $hcp \rightarrow bcc \rightarrow hcp \rightarrow fcc$, as a (nonmagnetic) transition metal series is traversed, has been shown to originate from the successive filling of a relatively narrow d band pinned at the Fermi level (E_F). By use of the so-called force theorem¹⁰ Skriver compared the total energies of the fcc, bcc, and hcp structures and successfully accounted for the crystal structures of all (except Au) nonmagnetic transition metals. In this study Skriver showed that for the determination of the energy differences between the fcc, bcc, and hcp structure the Madelung contribution to the total energy could be neglected and that the shape of

the d -partial density of states (DOS) in conjunction with the band filling was responsible for stabilizing a particular structure. As a matter of fact it was demonstrated that a potential and volume-independent quantity, the structure constant, which bears the structural information of the lattice, could be used to obtain the correct trend of the structures as the transition-metal series is traversed.^{7,8}

In this connection the occurrence of the ω phase in Ti, Zr, and Hf is most interesting since this structure is very open and from this point of view more related to the structures found among the p -electron systems or the actinide elements. A further similarity to the actinides is that the ω phase can be viewed as a distortion of the bcc structure. This is also the case in, for instance, both the β and α phases of Np (although here the crystal symmetry is lowered drastically). The main motivation for the present work is to investigate the reasons for the stability of the ω structure by means of accurate total-energy calculations.

Some theoretical work for these group-IV metals has already been published, in particular recent *ab initio*, zero-temperature total-energy calculations have been presented.¹¹ For Ti the ω phase was computed to be

lower in energy than the fcc, hcp, and bcc structures with ~ 10 – 15 mRy and it was also found that this structure was stable at all studied volumes.¹¹ For Zr it was found that the hcp structure is stable at ambient pressure, that at a pressure of 50 kbar the ω phase is stable, and that the bcc structure is stabilized at 110 kbar.¹¹ The correct crystal structure sequence of Zr as a function of pressure was thus obtained and the transition pressures were in good to fair agreement with experiment. Finally, for Hf the hcp structure was found to have the lowest energy at the experimental volume and the ω structure ~ 5 mRy higher in energy.¹¹ Under compression the calculations yield a hcp \rightarrow bcc transition at 510 kbar for Hf, which is slightly lower than the experimental value of 710 kbar for the appearance of the bcc phase. Also, the calculations presented in Ref. 11 did not give a stable ω phase at any compression for Hf, in disagreement with high-pressure experiments performed at room temperature. The spherical potential calculations presented in Ref. 11 thus yield results in rather good agreement with experiment for Zr whereas the results for Ti and Hf are more questionable. Furthermore, Ho *et al.*¹⁰ have made first-principle frozen phonon calculations and analyzed the basic reason for phonon anomalies and possible soft-mode phase transi-

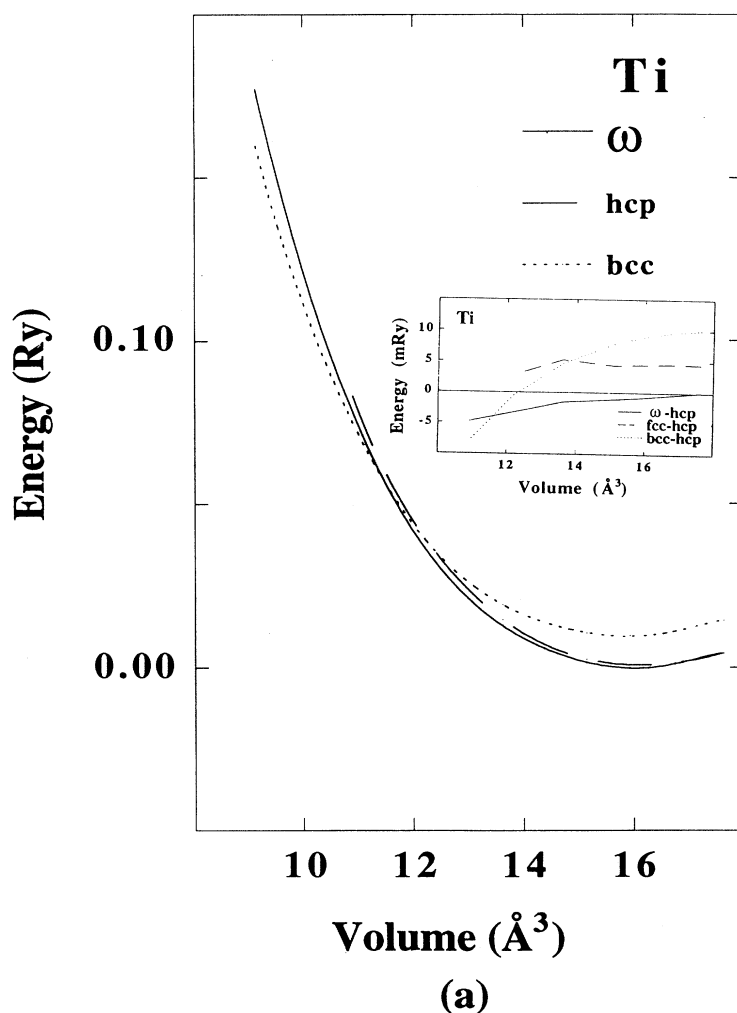


FIG. 1. Calculated total energy for Ti (a), Zr (b), and Hf (c), in the ω , hcp, and bcc structures. The inset shows the energy difference between these three structures. The energy of the hcp phase is here the reference level and is set equal to zero.

tions in Zr, Nb, and Mo. For a distortion associated with the bcc $L(\frac{2}{3}, \frac{2}{3}, \frac{2}{3})$ (L = longitudinal) phonon they found that the minimum in energy occurs when two of the (111) planes in the unit cell collapse into one common plane, thus forming the so-called ω phase. This leads to an instability of the bcc phase at low temperature. Further they have suggested that the $\text{bcc} \rightarrow \omega$ transition is first order in nature.

It is thus of interest to investigate if accurate zero-temperature calculations can reproduce the experimental results for the crystal structures of Ti, Zr, and Hf. We have therefore computed the total energies of these three metals as a function of volume and compared the total energies for the four crystal structures: fcc, bcc, hcp, and the ω phase. These calculations did not impose any geometrical restrictions on the charge density and potential (see below) and are based on the local-density approximation.

II. DETAILS OF THE CALCULATIONS

The calculations were based on the local-density approximation and we used the Hedin-Lundqvist¹² parame-

trization for the exchange and correlation potential. Basis functions, electron densities, and potentials were calculated without any geometrical approximation.¹³ These quantities were expanded in spherical waves (with a cutoff $l_{\text{max}} = 8$) inside nonoverlapping spheres surrounding the atomic sites (muffin-tin spheres) and in Fourier series in the interstitial region between the spheres. The muffin-tin spheres occupied approximately 35% of the unit-cell volume. This comparatively small spherical region was found necessary since the ω phase is quite open. The radial parts of the basis functions inside the muffin-tin spheres were calculated from a wave equation for the $l=0$ component of the potential inside the spheres that included mass velocity, Darwin, and higher-order corrections, but not spin-orbit coupling. Spin-orbit coupling and the higher l components of the potential in the muffin-tin spheres and all of the Fourier components of the potential in the interstitial region were included in the crystal Hamiltonian. For Ti and Zr, where spin-orbit effects are not important we neglected this term. For Hf we found it necessary to include the $4f$ states as "pseudo" valence states. The radial basis functions within the muffin-tin spheres, calculated as described above, are linear combinations of radial wave functions and their en-

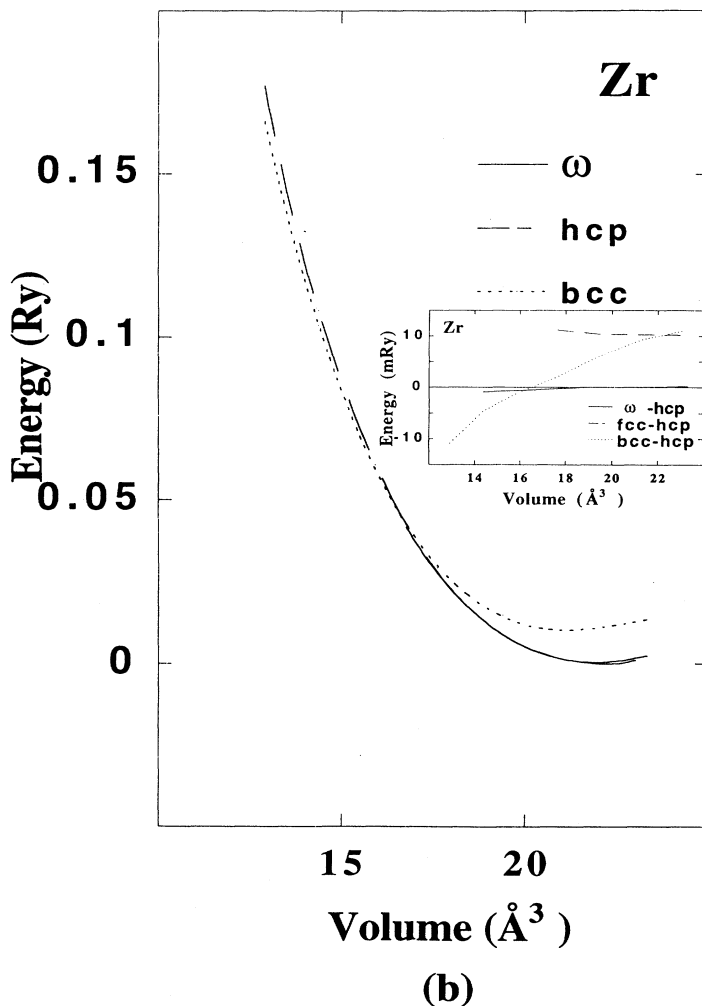


FIG. 1. (Continued).

ergy derivatives, calculated at energies appropriate to their site and principal as well as orbital atomic quantum numbers, whereas outside the muffin-tin spheres the basis functions are combinations of Neuman or Hankel functions.^{14,15} In the calculations reported here, two sets of energy parameters were used, one appropriate for the semicore p states, and the other appropriate for the valence states. The resulting bases formed a single, fully hybridizing basis set.

For sampling the irreducible wedge of the Brillouin zone we used the special k -point method,¹⁶ with 16 points for the ω structure, 76 k points for the hcp structure, 60 points for the fcc structure, and 58 points for the bcc structure. In addition to using the special k -point technique we have, in order to speed up the convergence of the k -point sampling, associated each calculated eigenvalue with a Gaussian function having a width ~ 15 mRy.

III. RESULTS

The total energy as a function of volume is presented for Ti (a), Zr (b), and Hf (c) in Fig. 1. The equilibrium volumes obtained from this figure are 16.0 \AA^3 , 22.2 \AA^3 , and 20.1 \AA^3 , for Ti, Zr, and Hf, respectively. This should

be compared with the experimental values 17.6 \AA^3 , 23.3 \AA^3 , and 22.3 \AA^3 for Ti, Zr, and Hf, respectively. Also, Fig. 1 shows that although the ω structure is more open than the hcp structure, the equilibrium volume of this phase is lower than for the hcp structure. This is in agreement with experiment for both Ti and Zr (for Hf there are no experimental values available).⁴ Also, for the three metals we find that the bcc structure, although not stable at zero pressure, has the lowest equilibrium volume. We have also included the energy differences between the various phases as a function of volume in the inset figure, with the hcp structure as the reference level. The most interesting feature is that for all three metals we calculate a crystallographic sequence $\text{hcp} \rightarrow \omega \rightarrow \text{bcc}$ with decreasing volume. The obtained transition pressures as well as the transition volumes are collected in Table I. For comparison, the experimental data for the various transitions are also quoted in Table I.

Starting with Ti we find that the hcp and ω structures have very similar energy (the hcp structure is only 0.06 mRy/atom lower in energy) at the experimental volume. This agrees rather well with experimental work at room temperature showing a transition to the ω phase at quite low pressures, and at only 2% compression. However, it

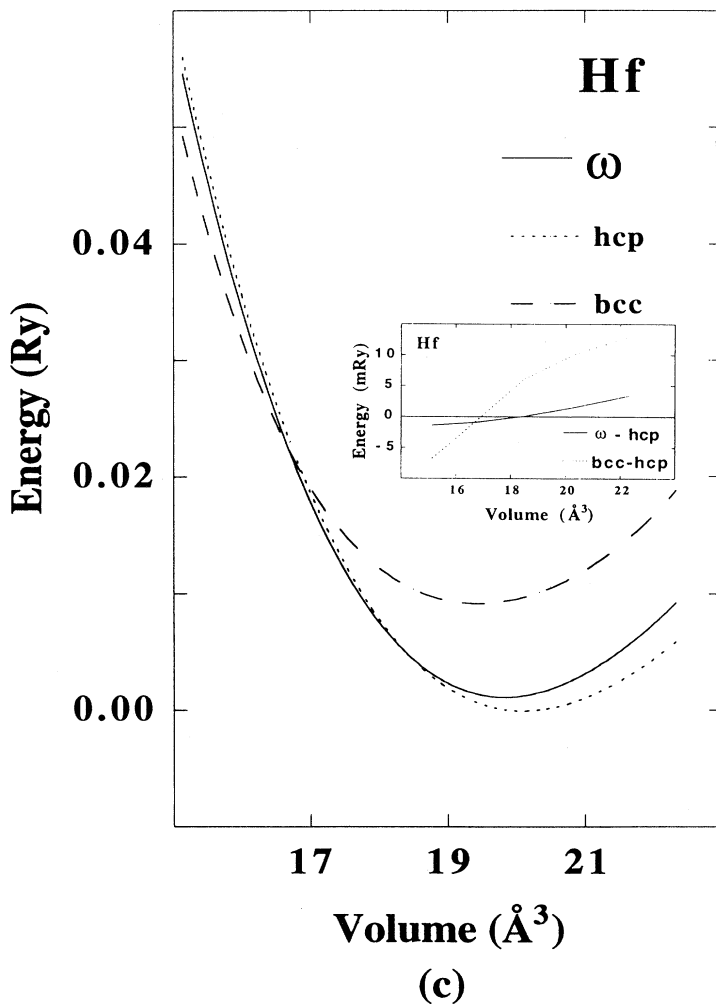


FIG. 1. (Continued).

may be noted that our calculations show that at the theoretical equilibrium volume the ω structure is slightly lower in energy than the hcp structure. This is in disagreement with room-temperature data which shows that the hcp structure is stable. On the other hand, the true crystal structure of Ti at zero temperature has not been determined experimentally and an extrapolation of the phase boundary between the ω and hcp structure give the ω phase stable. The bcc structure at high compression has not yet been observed in Ti, and our theoretical transition is therefore a prediction. However, previous experimental work reports the ω phase to be stable up to ~ 900 kbar, which is higher than our calculated transition pressure. Our theoretical value of 575 kbar for the onset of the bcc structure in Ti is therefore in disagreement with the experimental data reported in Ref. 5. Next, for Zr we reproduce the experimental trend,

TABLE I. Theoretical and experimental data for the transition pressures (kbar) of the ω and bcc structures. The corresponding volumes (relative to the experimental equilibrium volume V_0) are also tabulated.

	Ti	Zr	Hf
$P_{\text{hcp} \rightarrow \omega}^{\text{expt}}$	20–80 ^a	20–60 ^b	380 ^c
$P_{\text{hcp} \rightarrow \omega}^{\text{theo}}$	~ 0	~ 0	139
$V_{\text{hcp} \rightarrow \omega}^{\text{expt}}$	0.98 ^a	0.977 ^b	0.78 ^c
$V_{\text{hcp} \rightarrow \omega}^{\text{theo}}$	~ 1	~ 1	0.82
$P_{\omega \rightarrow \text{bcc}}^{\text{expt}}$		300 ^c	710 ^c
$P_{\omega \rightarrow \text{bcc}}^{\text{theo}}$	575	483	307
$V_{\omega \rightarrow \text{bcc}}^{\text{expt}}$		0.764 ^b	0.69 ^c
$V_{\omega \rightarrow \text{bcc}}^{\text{theo}}$	0.66	0.69	0.74

^aReferences 3, 4, and 5.

^bReferences 3 and 5.

^cReference 5.

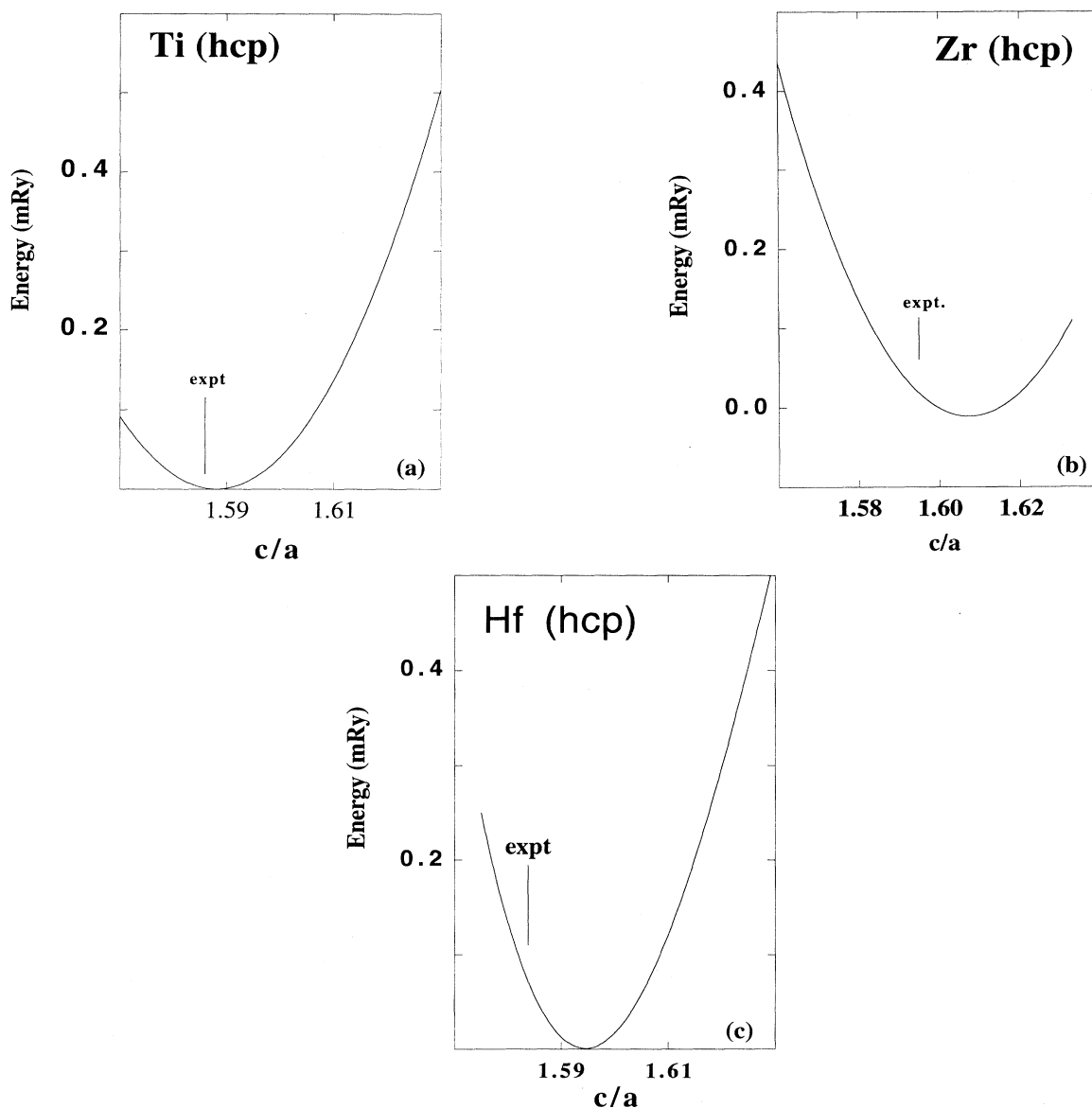


FIG. 2. Calculated total energy as a function of c/a , for hcp Ti (a), hcp Zr (b), and hcp Hf (c).

hcp $\rightarrow\omega\rightarrow$ bcc, as a function of pressure, and the transition pressures as well as transition volumes agree rather well with experimental data. Experiments show that the energy difference between the hcp and ω structures is small, since the transition pressure from hcp to ω is only 20 kbar and the transition shows hysteresis. As a matter of fact it is possible to stabilize Zr in the ω structure at zero pressure by first applying a pressure and then releasing it. This is consistent with our finding of the hcp structure being only 0.2 mRy/atom lower in energy at the experimental volume. For the compressed bcc structure the calculations overestimate the transition pressure and correspondingly underestimate the transition volume. Finally, in the case of Hf our calculations show the largest disagreement with experiment. Although the correct crystal structure trend, hcp $\rightarrow\omega\rightarrow$ bcc, is obtained, we calculate too low transition pressures both for the hcp $\rightarrow\omega$ structure as well as for $\omega\rightarrow$ bcc crystal change.

Next, we investigated the c/a ratio for the hcp structure for Ti, Zr, and Hf, as well as the c/a ratio of the ω phase of Zr. To illustrate this we display in Fig. 2 the calculated energy as a function of the c/a ratio for hcp Ti (a), Zr (b), and Hf (c), as well as the total energy as a function of c/a in the ω structure for Zr in Fig. 3. The c/a values which give a minimum total energy are listed in Table II together with experimental data. Notice that the agreement between experiment and theory is very good, not least for the ω phase. It is also clear from Figs. 2 and 3 that the total energy changes relatively slowly with c/a for these systems.

IV. ELECTRONIC STRUCTURE AND CHARGE DENSITY

We now turn to the basic reason for the crystal structure sequence hcp $\rightarrow\omega\rightarrow$ bcc with increasing pressure and

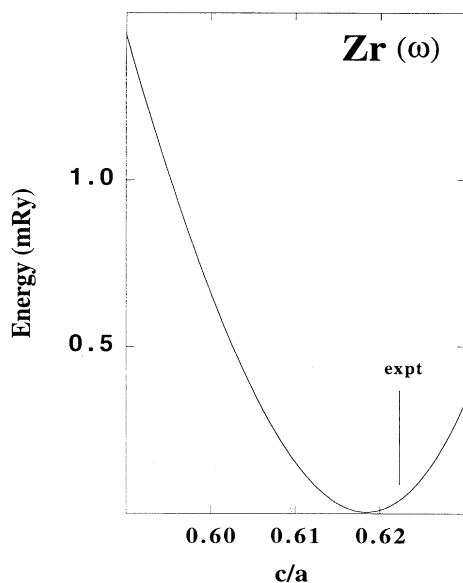


FIG. 3. Calculated total energy as a function of c/a , for the ω phase in Zr.

TABLE II. Theoretical and experimental c/a data for hcp Ti, Zr, and Hf as well as for the c/a ratio for ω Zr.

	Ti	Zr	Hf
$c/a_{\text{hcp}}^{\text{expt}}$	1.588 ^a	1.593 ^a	1.582 ^a
$c/a_{\text{hcp}}^{\text{theo}}$	1.588	1.606	1.594
$c/a_{\omega}^{\text{expt}}$		0.625 ^b	
$c/a_{\omega}^{\text{theo}}$		0.617	

^aReference 1.

^bReference 5.

in connection to this we present charge-density contour plots, orbital occupation numbers, and the electronic structure. For brevity we will concentrate on Zr. Thus, in Fig. 4 we present the density of states (DOS) for Zr in the hcp, ω , and bcc structure at the equilibrium volume, i.e., $V/V_0 = 1.0$ where V_0 is the experimental volume (a), as well as the DOS at $V/V_0 \sim 0.69$ (b), i.e., at a volume where the bcc structure is stable. Notice in Fig. 4 that for all the three structures the occupied part of the energy band complex is only slightly broader for the lower volumes, whereas the d DOS is substantially broader. Since the bottom of the band is of s character and since this band moves up in energy with decreasing volume, the width of the occupied part of the band stays almost constant although the total bandwidths broaden. Notice also in Fig. 4 that at higher volumes the eigenvalue sum for the occupied levels stabilizes the hcp and ω phases over the bcc structure, since the DOS of the hcp and ω structures have most weight at energies below the Fermi level (E_F), in contrast to the DOS of the bcc structure for which there is a peak pinned at E_F . In contrast, at low volumes the peak found in the bcc structure has been filled and now E_F lies in a region with low density of states, and correspondingly the eigenvalue sum stabilizes the bcc structure over both the hcp and the ω structure. The general trend of the crystal structures of these elements as a function of pressure can thus be understood using the same arguments as Duthie and Pettifor,⁸ as well as Skriver,⁷ used for understanding the trends of the crystal structures of the transition metals at ambient pressure. Namely, that the one-electron contribution to a large extent determines the stabilization of the crystal structures.

The arguments presented above are based on the fact that the shape of the DOS as well as the filling of the one-electron levels are modified when the volume is changed. Normally one tries to correlate the stability of certain structures with the d occupation. However, with the presently used basis functions an analysis based upon orbital occupations can be somewhat misleading. To illustrate this we display in Fig. 5 the orbital occupation numbers for hcp, bcc, and ω Zr as a function of volume. Notice that the d occupation is essentially independent of volume whereas the interstitial change is increasing with decreasing volume. The reason for this behavior is that in our calculations we have modified the muffin-tin radius so that the fraction of the volume occupied by the muffin-tin radii is the same for all volumes, and this makes the l projected charge density an ill-defined quanti-

ty when comparisons are made for different volumes. Furthermore, Fig. 5 shows a large difference in d occupation for atom 1 and 2 in the ω phase (atom 2 is situated in the more densely packed plane and atom 1 in the more open plane). It can also be noticed that the d occupation for atom 1 is increasing with decreasing volume whereas for atom 2 it is almost constant. For the hcp and the bcc phase the d occupation shows a slightly increasing trend with decreasing volume. Finally the d occupations for the hcp, bcc, and ω (atom 2) phases are very similar to each other.

In order to further study the one-electron contribution to the stabilization of the different structures we proceed with an analysis which has previously been made for the hcp, fcc, and bcc structure stabilities of the transition metals. Namely, we study the canonical d bands of the presently investigated structures. In particular we

display the eigenvalue sum for the three structures as a function of the d -band filling in Fig. 6. Notice that for all band fillings the eigenvalue sum of the canonical bands stabilizes the ω structure, except for band fillings of $\sim 3-5$ where the bcc structure is stable. For d occupations around 2, as well as for d occupations between 6 and 8, Fig. 6 suggests a particularly strong favorization of the ω structure. However, there is of course an opposing effect, namely the Madelung contribution, which tends to stabilize the close-packed structures. For Ti, Zr, and Hf where the d occupation is close to 2 these two effects are apparently producing a total energy which is approximately the same for the hcp, bcc, and ω structures.

The canonical one-electron energies in Fig. 6 suggest that the ω structure might also exist for other band fillings and in particular for d -band fillings close to 6-8. In the $4d$ series this corresponds to Tc and Ru and we

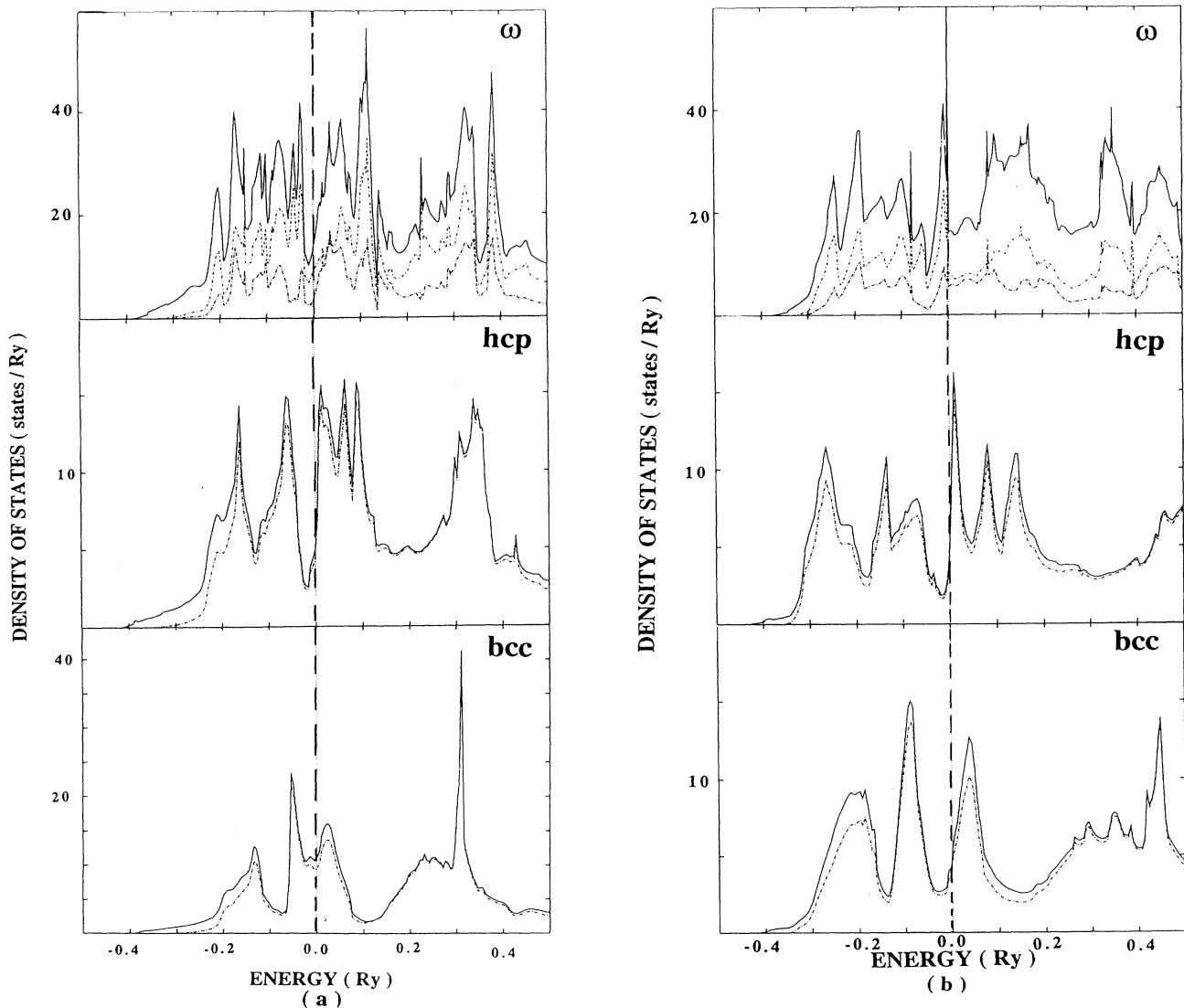


FIG. 4. DOS for the bcc, hcp, and ω phases at the experimental volume (a) and at a compressed volume (b). In each panel the upper curve is the total DOS and the dotted curves the d -partial DOS. For the ω structure there are two atom types and therefore we have plotted the d -partial DOS for both atoms.

have therefore performed fully self-consistent linear-muffin-tin-orbital-atomic-sphere-approximation (ASA) (Refs. 14 and 15) calculations for these two elements. Using the force theorem¹⁰ we then computed the energy difference between the hcp and ω structure and we found the hcp phase to be stable. The ω phase was 20 mRy/atom higher in Tc and 18 mRy/atom higher in Ru. It thus seems that Ti, Zr, and Hf are unique in the sense of having the ω structure competing with the structures normally found in transition metals (fcc, hcp, and bcc).

Next we discuss the character of the chemical bonds in the different structures. In Fig. 7 we show the charge

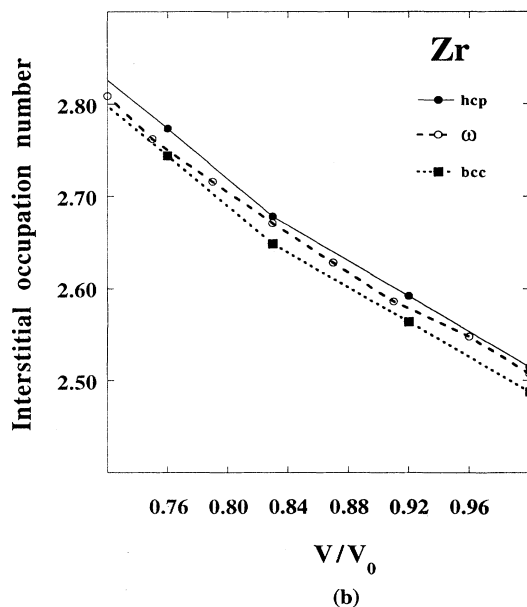
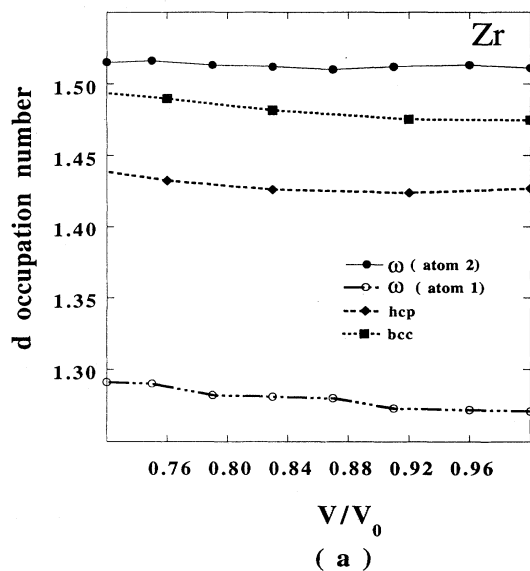


FIG. 5. (a) Calculated d occupation number for Zr in the ω , hcp, and bcc structures as a function of volume. (b) Calculated interstitial occupation number for Zr in the ω , hcp, and bcc structures as a function of volume.

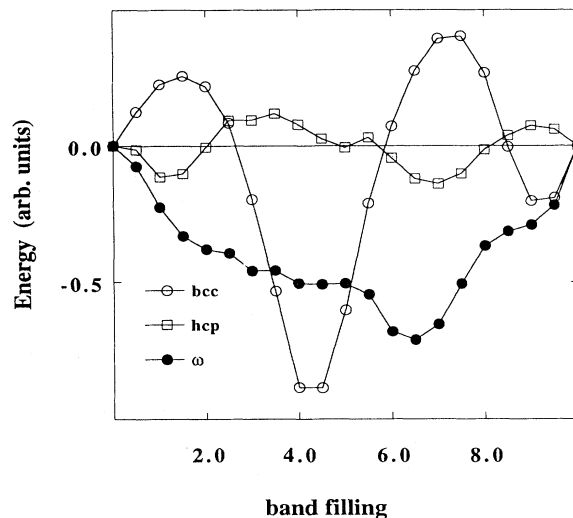


FIG. 6. Energy differences obtained from canonical d bands as a function of the d -band filling for the hcp (open squares), bcc (open circles), and ω (filled circles) structures. The fcc (solid line) phase is used as the reference level and is set equal to zero.

densities for the bcc, hcp, and ω structures. The density for the bcc structure is shown for a cut in the (100) plane, whereas for the ω and hcp structures the cut is shown for the (0001) plane (at $z=0$). Notice that the change densities for the hcp and bcc structures are quite similar, with spherical regions around the atomic sites, and more or less flat regions in the interstitial region. The situation is quite different for the ω structure where the density shows a large degree of nonspherical behavior, indicating covalent bonds. For instance, between the three atomic positions [of atom type (1)] there is an increase of charge yielding a triangular shape of the density contours. This reflects the fact that there is an atom [of atom type(2)] situated at this (x,y) position but one plane up (at $z=c/2a$). There are also covalent bonds between this atom and the atoms in the $z=0$ plane, and this is reflected by an increase of charge between the atoms at $z=0$ and the triangular-shaped contour. The chemical bonding for the ω structure is thus quite different from what one normally finds in transition metals, with a larger degree of covalency.

V. MECHANICAL STABILITY OF THE bcc CRYSTAL STRUCTURE

At zero pressure and high temperature all the group-IV B elements transform from the hcp to the bcc crystal structure. In Sec. III we have calculated that also at zero temperature and high pressure all three metals will enter in the bcc phase. Therefore it might be that there is contact between these two bcc regions in the (P,T) phase diagram. However, at zero temperature we have found a crystal structure sequence $\text{hcp} \rightarrow \omega \rightarrow \text{bcc}$ with compression and the group-IV B phase diagrams are therefore made more complex by the presence of the intermediate ω phase. In Fig. 8 we present a possible schematic phase diagram for these tetravalent metals.

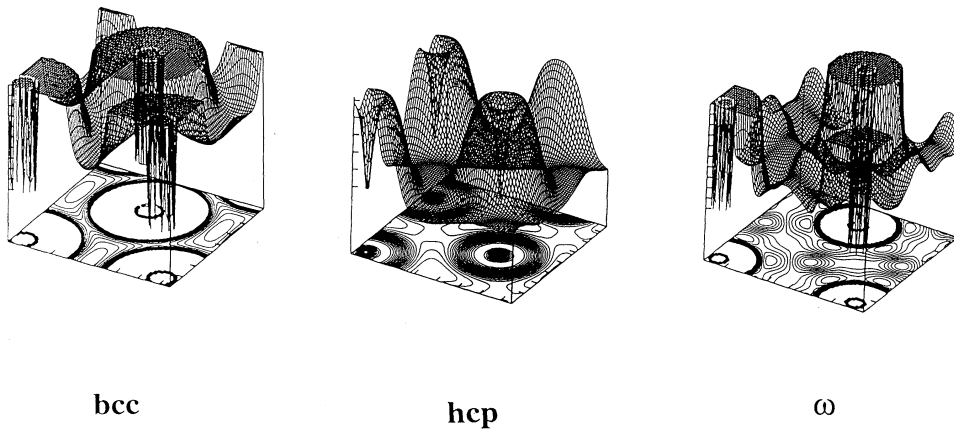


FIG. 7. Charge density for the bcc, hcp, and ω structures in Zr. The bcc contour is from a cut in the (001) plane, the hcp contour is from a cut in the (0001) plane, and the ω contour is from a cut in the (0001) plane. The logarithm of the density is shown, and the density has been cut off above a certain level.

It turns out to be very interesting to investigate the local stability of the bcc phase. In Fig. 9 we show the calculated behavior of the total energy for Hf along the Bains path.¹⁷ This path is a deformation of the bcc phase where a tetragonal distortion is introduced and studied as a function of the axis ratio (c/a) for a constant volume. For $c/a=1.0$ this corresponds to the bcc structure and for $c/a=\sqrt{2}$ it is the fcc structure. For a volume reduction of $V/V_0=0.45$, i.e., at a volume for which the bcc structure is calculated to have the lowest energy, we find that the total energy indeed has a minimum for $c/a=1.0$. In sharp contrast to this, at the zero-pressure volume $V/V_0=1.0$ we calculate a local maximum in the energy curve $E=E(c/a)$ at $c/a=1.0$. Since the curvature of $E(c/a)$ around $c/a=1.0$ directly corresponds to C' [$C'=\frac{1}{2}(C_{11}-C_{12})$ where C_{11} and C_{12} are elastic constants], this means a negative value of C' and a mechanically unstable situation. Therefore we observe that C' will change sign with pressure. For Hf this change of sign takes place at a volume $V/V_0=0.80$. The calculat-

ed volume dependence of C' for Ti, Zr, and Hf is shown in Fig. 10. We notice that for the high-pressure bcc phase, the calculated C' values are all positive, in agreement with the observed high-pressure bcc phase in Zr and Hf. This can be understood as an effect of the $s \rightarrow d$ transfer, since under pressure the d occupation of a given element, say Zr, is increasing, making it behave more like its nearest-neighbor element Nb, which has the bcc crystal structure.

It is thus of considerable interest to notice that the bcc phase at ambient volumes is calculated to be mechanically unstable. Despite this severe instability, the bcc crystal structure is observed experimentally at high temperature in all three metals. This has to be explained as an effect of the high entropy associated with the bcc phase. Thus we have to conclude that the bcc structure is stabilized due to the phononic behavior at high temperature. Therefore the high-temperature bcc structure for these three elements must show anomalous properties. An ex-

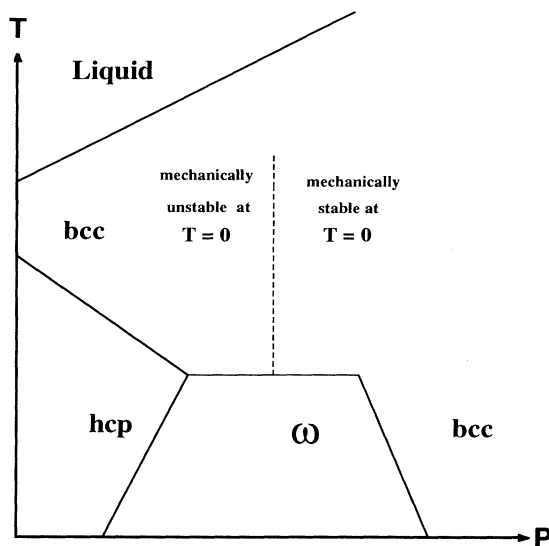


FIG. 8. Schematic phase diagram for Ti, Zr, and Hf. P denotes pressure and T denotes temperature.

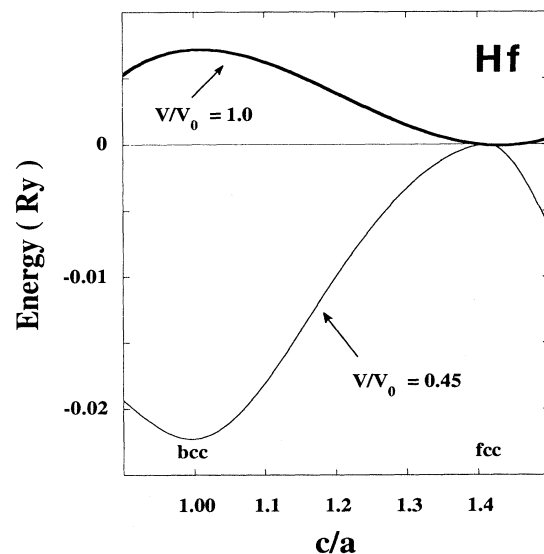


FIG. 9. Energy along the Bains path for Hf at the experimental volume ($V/V_0=1.0$) as well as for a compressed volume ($V/V_0=0.45$).

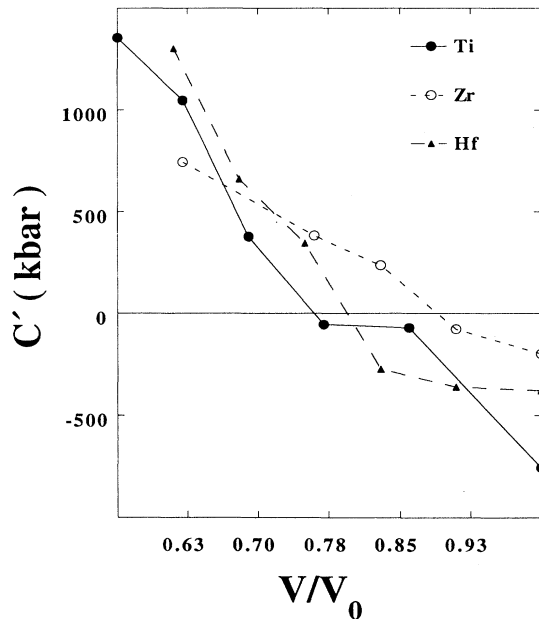


FIG. 10. Calculated tetragonal shear constant (C') as a function of relative volume for Ti, Zr, and Hf in the bcc phase.

ample of this is the experimental observation that within the bcc phase these three metals become increasingly stiff with increasing temperature,¹⁸⁻²¹ a most unusual behavior. For a different type of deformation of the bcc Zr lattice, Ye *et al.*²² also found a mechanical instability and by introducing anharmonic effects they could show that at high temperatures the bcc crystal structure becomes stabilized.²³

The observed anomalous diffusion properties of these three metals in the bcc phase might be related to the intrinsic mechanical instability corresponding to C' .²⁴ Another possible explanation for their exceptional diffusion property has been proposed,²⁵ namely that an intermediate state in the diffusion process might be related to the ω phase. The fact that the ω phase is calculated to have lower total energy than the bcc phase at the equilibrium volume V_0 for all three metals also gives support to such an interpretation.

In the (P, T) phase diagram the phase line between the hcp and bcc phase has a negative slope.²⁶ This might be related to the fact that we calculate a decreasing magnitude of the negative C' with decreasing volume. Thus the mechanical instability becomes less severe with increasing pressure and therefore a lower temperature is needed to restore the stability of the bcc crystal structure. In addition we calculate a smaller equilibrium volume for the bcc structure than for the hcp structure (cf. Fig. 1).

To obtain the elastic constant C_{44} we perform total-energy calculations for the appropriate deformations of the bcc crystal structure. In Table III we compare experimental data for C_{44} in the high-temperature bcc phase for Ti, Zr, and Hf with our results. As we can see the agreement is very good. Thus it appears that the shear corresponding to C' has to be very strongly modified by

TABLE III. Theoretical and experimental C_{44} (kbar) for bcc, Ti, Zr, and Hf.

	Ti	Zr	Hf
$C_{44}^{\text{expt}}_{\text{bcc}}$	360 ^a	380 ^b	450 ^c
$C_{44}^{\text{theo}}_{\text{bcc}}$	358	328	440

^aReference 19.

^bReference 20.

^cReference 21.

phonons since the bcc structure has become stable at high temperature, while C_{44} appears to be very much unaffected by temperature.

VI. SUMMARY

In summary we have reproduced the experimental trend of a crystallographic sequence: hcp \rightarrow ω \rightarrow bcc with pressure for Zr and Hf. For Ti at the experimental volume we obtain the hcp structure marginally more stable than the ω phase whereas at the theoretical equilibrium volume we calculate the energy of the ω structure to be slightly lower in energy than the hcp structure. Also, we predict that Ti should stabilize in the bcc structure at high pressures. Our calculated transition pressures deviate from experiment by as much as ~ 400 kbar for the bcc structure in Hf and we have no explanation for this rather large discrepancy. On the other hand, the calculated transition volume ($V/V_0 = 0.74$) is not too different from the experimental value ($V/V_0 = 0.69$). For Zr the agreement with experiment is better. The internal crystallographic parameters agree very well with experiment both for the hcp structure of Ti, Zr, and Hf as well as for the ω structure of Zr. It should be noted here that our calculations are at zero temperature whereas the experimental work has been done at room temperature. Some of the disagreement between experiment and theory might be due to thermal effects. For instance, our calculations predict Ti to have the lowest energy in the ω structure (which is slightly lower in energy than the hcp structure), whereas the room-temperature experiments show that the structure is hcp. However, extrapolating the experimental phase boundary between the hcp and ω structure actually gives the ω phase stable and it would be interesting if experimental work could determine the low-temperature region of the Ti phase diagram.

The charge density for the ω phase is found to have a substantial nonspherical component reflecting covalent bonding. This is quite different from the chemical bonding found in the fcc, hcp, and bcc structures where the charge density is highly spherical around the atomic positions and flat in the interstitial. The chemical bonding for these latter structures is metallic. Despite the difference in the character of the chemical bonds for the various structures (more covalent for the ω phase relative to the bcc, fcc, and hcp phases) we can to some extent use band-filling arguments to explain the crystallographic sequence of these metals. Also the zero-pressure bcc crys-

tal structure is shown to be highly anomalous, since at zero temperature this structure is found to be unstable against several types of distortions. This is certainly related to the fact that the high-temperature bcc phase is known to exhibit several anomalous properties.

Finally, we failed to obtain a stable ω structure in Tc and Ru. Instead the hcp structure was found to be sub-

stantially lower in energy, in agreement with experiments.

ACKNOWLEDGMENT

Valuable discussions with P. Söderlind, G. H. Lander, and M. R. Norman are acknowledged.

- ¹J. Donohue, *The Structure of the Elements* (Wiley, New York, 1974), Chap. 6.
- ²A. R. Kutzar, *Pis'ma Zh. Eksp. Teor. Fiz.* **35**, 91 (1982) [*JETP Lett.* **35**, 108 (1982)].
- ³S. K. Sikka, Y. K. Vohra, and R. Chidambaram, *Prog. Mater. Sci.* **27**, 245 (1982).
- ⁴J. C. Jamieson, *Science* **140**, 72 (1963); A. Jayaraman, W. Clement, and G. C. Kennedy, *Phys. Rev.* **131**, 644 (1963).
- ⁵H. Xia, G. Parthasarathy, H. Luo, Y. K. Vohra, and A. L. Ruoff, *Phys. Rev. B* **42**, 6736 (1990); H. Xia, S. J. Duclos, A. L. Ruoff, and Y. K. Vohra, *Phys. Rev. Lett.* **64**, 204 (1990).
- ⁶K. M. Ho, C. L. Fu, B. N. Harmon, W. Weber, and D. R. Hamann, *Phys. Rev. Lett.* **49**, 673 (1982).
- ⁷H. L. Skriver, *Phys. B* **31**, 1909 (1985).
- ⁸J. C. Duthie and D. G. Pettifor, *Phys. Rev. Lett.* **38**, 564 (1977).
- ⁹B. Johansson and A. Rosengren, *Phys. Rev. B* **11**, 2836 (1975).
- ¹⁰D. G. Pettifor, *Commun. Phys.* **1**, 141 (1976); D. G. Pettifor, J. Chem. Phys. **69**, 2930 (1978); A. R. Mackintosh and O. K. Andersen, in *Electrons at the Fermi Surface*, edited by M. Springford (Cambridge University Press, Cambridge, 1980).
- ¹¹J. S. Gyanchandani, S. C. Gupta, S. K. Sikka, and R. Chidambaram, in *Shock Compression of Condensed Matter*, edited by S. C. Schmidt, J. N. Johnson, and L. W. Davidson (Elsevier, Amsterdam, 1990); *J. Phys. Condens. Matter* **2**, 6457 (1990); **2**, 301 (1990).
- ¹²L. Hedin and B. I. Lundqvist, *J. Phys. C* **4**, 2064 (1971).
- ¹³J. M. Wills (unpublished); J. M. Wills and B. R. Cooper, *Phys. Rev. B* **36**, 3809 (1987); D. L. Price and B. R. Cooper, *ibid.* **39**, 4945 (1989).
- ¹⁴O. K. Andersen, *Phys. Rev. B* **12**, 3060 (1975).
- ¹⁵H. L. Skriver, *The LMTO Method* (Springer, Berlin, 1984).
- ¹⁶D. J. Chadi and M. L. Cohen, *Phys. Rev. B* **8**, 5747 (1973); S. Froyen, *ibid.* **39**, 3168 (1989).
- ¹⁷I. C. Bain, *Trans AIME* **70**, 25 (1924).
- ¹⁸G. Grimvall, in *Transition Metals*, edited by M. J. G. Lee, J. M. Perz, and E. Fawcett, IOP Conf. Proc. No. 39 (Institute of Physics and Physical Society, London, 1978), p. 174.
- ¹⁹W. Petry, A. Heiming, J. Trampenau, M. Alba, C. Herzig, H. R. Schober, and G. Vogl, *Phys. Rev. B* **43**, 10 933 (1991).
- ²⁰A. Heiming, W. Petry, J. Trampenau, M. Alba, C. Herzig, H. R. Schober, and G. Vogl, *Phys. Rev. B* **43**, 10 948 (1991).
- ²¹J. Trampenau, A. Heiming, W. Petry, M. Alba, C. Herzig, W. Miekeley, and H. R. Schober, *Phys. Rev. B* **43**, 10 963 (1991).
- ²²Y.-Y. Ye, Y. Chen, K. M. Ho, B. N. Harmon, and P.-A. Lindgård, *Phys. Rev. Lett.* **58**, 1769 (1987).
- ²³K. M. Ho and B. N. Harmon, *Mater. Sci. Eng. A* **127**, 155 (1990).
- ²⁴A possible diffusion path for a bcc atom at position $(\frac{1}{2}, \frac{1}{2}, \frac{1}{2})$ into a vacancy at $(-\frac{1}{2}, \frac{1}{2}, \frac{1}{2})$ goes through the position $(0, \frac{1}{2}, \frac{1}{2})$. This is a fcc-like position in the $(0, y, z)$ plane. In Fig. 9 we found that for $V=V_0$ the fcc crystal energy is considerably lower than for the bcc phase, suggesting that such a diffusion path is associated with a low activation energy.
- ²⁵J. M. Sanchez and D. de Fontaine, *Phys. Rev. Lett.* **35**, 227 (1975).
- ²⁶D. A. Young, *Phase Diagrams of The Elements* (University of California Press, Berkeley, 1991).